Gene Regulation:

Physical and Functional Interactions between the Histone H3K4 Demethylase KDM5A and the Nucleosome Remodeling and Deacetylase (NuRD) Complex

Gohei Nishibuchi, Yukimasa Shibata, Tomohiro Hayakawa, Noriyo Hayakawa, Yasuko Ohtani, Kaori Sinmyozu, Hideaki Tagami and Jun-ichi Nakayama

J. Biol. Chem. 2014, 289:28956-28970.
doi: 10.1074/jbc.M114.573725 originally published online September 4, 2014

THE JOURNAL OF BIOLOGICAL CHEMISTRY VOL. 289, NO. 42, pp. 28956–28970, October 17, 2014

Physical and Functional Interactions between the Histone H3K4 Demethylase KDM5A and the Nucleosome Remodeling and Deacetylase (NuRD) Complex*[S]

Received for publication, April 14, 2014, and in revised form, August 17, 2014 Published, JBC Papers in Press, September 4, 2014, DOI 10.1074/jbc.M114.573725

Gohei Nishibuchi[‡], Yukimasa Shibata[§], Tomohiro Hayakawa[¶], Noriyo Hayakawa[¶], Yasuko Ohtani[¶], Kaori Sinmyozu[‖], Hideaki Tagami[‡], and Jun-ichi Nakayama[‡¶1]

From the [‡]Graduate School of Natural Sciences, Nagoya City University, Nagoya 467-8501, the [§]Department of Bioscience, Graduate School of Science and Technology, Kwansei-Gakuin University, Sanda, Hyogo 669-1337, and the [¶]Laboratory for Chromatin Dynamics and [‖]Proteomics Support Unit, RIKEN Center for Developmental Biology, Kobe 650-0047, Japan

Background: Dynamic changes in histone modifications and chromatin structure are tightly linked to transcriptional regulation.
Results: KDM5A, a histone H3K4 demethylase, physically interacts with the nucleosome remodeling and deacetylase (NuRD) complex.
Conclusion: KDM5A and the NuRD complex cooperatively function to control developmentally regulated genes.
Significance: Elucidating the functional interplay between histone-modifying enzymes and chromatin remodeling machineries helps clarify development-related gene regulation.

Histone H3K4 methylation has been linked to transcriptional activation. KDM5A (also known as RBP2 or JARID1A), a member of the KDM5 protein family, is an H3K4 demethylase, previously implicated in the regulation of transcription and differentiation. Here, we show that KDM5A is physically and functionally associated with two histone deacetylase complexes. Immunoaffinity purification of KDM5A confirmed a previously described association with the SIN3B-containing histone deacetylase complex and revealed an association with the nucleosome remodeling and deacetylase (NuRD) complex. Sucrose density gradient and sequential immunoprecipitation analyses further confirmed the stable association of KDM5A with these two histone deacetylase complexes. KDM5A depletion led to changes in the expression of hundreds of genes, two-thirds of which were also controlled by CHD4, the NuRD catalytic subunit. Gene ontology analysis confirmed that the genes commonly regulated by both KDM5A and CHD4 were categorized as developmentally regulated genes. ChIP analyses suggested that CHD4 modulates H3K4 methylation levels at the promoter and coding regions of target genes. We further demonstrated that the *Caenorhabditis elegans* homologues of KDM5 and CHD4 function in the same pathway during vulva development. These results suggest that KDM5A and the NuRD complex cooperatively function to control developmentally regulated genes.

A strict regulation of gene expression patterns is essential for cellular differentiation during development. Control of gene expression is tightly linked to the chromatin structure, which is dynamically regulated by the combined actions of histone-modifying enzymes and chromatin remodeling machineries. KDM5A (also known as RBP2 or JARID1A) was first identified as a factor that interacts with the retinoblastoma gene product (RB) (1), and it has been shown to be involved in diverse biological processes such as cellular differentiation (2, 3), senescence (4, 5), tumorigenesis (6–8), circadian oscillation (9), and mitochondrial biogenesis (10). KDM5A is a member of the four KDM5 protein family, which also includes KDM5B (PLU-1/JARID1B), KDM5C (SMCX/JARID1C), and KDM5D (SMCY/JARID1D), all of which are associated with development and disease (11–16). Although mammals have four KDM5 family members, other organisms have only one homologue; the homologues in *Drosophila* (LID) and in *Caenorhabditis elegans* (RBR-2) also play critical roles in developmental processes (17–21).

KDM5 family members contain an evolutionarily conserved JmjC domain and were found to possess histone demethylase activities that target histone H3 lysine 4 (3, 11, 14, 17, 22). As trimethylation at this site (H3K4me3) is highly associated with transcriptional start sites of actively transcribed genes, KDM5 members are thought to regulate the expression of genes encoding developmental regulators. It is widely accepted that the histone-modifying enzymes are assembled into multisubunit complexes that enable the coordinated action of distinct activities to efficiently regulate chromatin remodeling (23, 24). Human KDM5A has been identified in SIN3B-containing histone deacetylase (HDAC)[2] complexes (22), suggesting that its demethylation activity is tightly linked with histone deacetylation processes. The SIN3B-HDAC complex also contains MRG15, a chromodomain protein that binds to H3 methylated

* This work was supported by grants-in-aid from the Ministry of Education, Culture, Sports, Science, and Technology of Japan.
[S] This article contains supplemental Table S1.
[1] To whom correspondence should be addressed: Graduate School of Natural Sciences, Nagoya City University, 1 Yamanohata, Mizuho-cho, Mizuho-ku, Nagoya, 467-8501, Japan. Tel./Fax: 81-52-872-5866; E-mail: jnakayam@nsc.nagoya-cu.ac.jp.

[2] The abbreviations used are: HDAC, histone deacetylase; NuRD, nucleosome remodeling and deacetylase; Muv, multivulva; IP, immunoprecipitate; TSS, transcriptional start site; qRT, quantitative RT; synMuv, synthetic multivulva.

at lysine 36 (H3K36me) (25), implying functional interplay between H3K4me3 and H3K36me. In *Drosophila*, the KDM5 homologue LID forms two distinct complexes with dSIN3, RLAF and LAF, and each complex functions with histone chaperones, NAP1 and ASF1, respectively, to silence NOTCH-regulated genes (26). Because human KDM5A is involved in diverse biological processes, it is likely that KDM5A functions cooperatively with other chromatin-modulating factors to regulate gene expression during developmental processes.

The nucleosome remodeling and histone deacetylation (NuRD) complex mediates transcriptional repression by regulating chromatin structure in mammalian cells (27). The NuRD core complex consists of HDAC1/2, histone-binding protein RbAp46/48, ATP-dependent chromatin remodeler Mi-2α/β (CHD3/CDH4), metastasis-associated factor (MTA1/MTA2/MTA3), methyl-DNA-binding protein (MBD2/MBD3), and GATAD2 (24, 28). This complex has both histone deacetylation and nucleosome remodeling activities (29–32) and functions together with other transcriptional regulators in developmental processes (33, 34) and tumorigenesis (35).

Here, we report the physical and functional association of human KDM5A and the NuRD complex. A proteomic survey of proteins that interact with KDM5A revealed that KDM5A stably associates with two distinct HDAC complexes, the SIN3B-containing HDAC and NuRD complexes. Comparison of gene expression changes in cells depleted of KDM5A or the NuRD complex component, CHD4, showed that hundreds of developmentally regulated genes are shared targets of KDM5A and CHD4. The cooperative functioning of KDM5 and the NuRD complex was also confirmed in *C. elegans* vulva development. Our results provide a conserved molecular mechanism for the interplay of histone demethylation and ATP-dependent chromatin remodeling.

EXPERIMENTAL PROCEDURES

Cell Culture—T-Rex HeLa (Invitrogen) and MCF7 cells were cultured in minimum Eagle's medium (Nacalai Tesque) supplemented with 1 mM sodium pyruvate (Invitrogen). HeLa (CCL-2; ATCC), HEK293T, and U2OS cells were cultured in DMEM (Nacalai Tesque). All culture media were supplemented with 10% fetal calf serum (Invitrogen). T-Rex HeLa cells expressing tetracycline-inducible FLAG-KDM5A were selected and maintained in medium containing 100 μg/ml Zeocin (Invitrogen). T-Rex HeLa cells expressing tetracycline-inducible 3×FLAG-tagged MRG15, EMSY, or ZMYND8 were selected in medium containing 2 μg/ml puromycin (Invivogen), and isolated clones were maintained in medium containing 1 μg/ml puromycin.

Antibodies—The antibodies used in this study were as follows: anti-histone H3 (ab1791, Abcam); anti-H3K4me3 (MABI0304, MAB Institute, Inc.); anti-H3K4me2 (MABI0303, MAB Institute, Inc.); anti-H3K36me3 (MABI0333, MAB Institute, Inc.); anti-FLAG M2 (Sigma); anti-KDM5A (Bethyl, A300-897A, Bioacademia: 9A6, 18E8); anti-KDM5B (HPA027179: Sigma); anti-KDM5C (39229, Active motif); anti-EMSY (ab19164, Abcam); anti-HDAC2 (ab1770, Abcam); anti-RbAp46 (4522, Cell Signaling); anti-RbAp48 (R3654, Sigma); anti-SIN3B (SC-768, Santa Cruz Biotechnology); anti-PF1 (NB100-81671, Novus); anti-ZMYND8/PRKCBP1 (H00023613, Abnova); anti-CHD4 (H00001108, Abnova), anti-MTA2 (M1194, Sigma), anti-GATAD2A (HPA006759, Sigma), anti-KDM1A/LSD1 (07–705, Millipore); and anti-TUBULIN (T5168, Sigma). Anti-MRG15 rabbit polyclonal antibodies were previously described (22). Anti-KDM5A rabbit polyclonal antibodies were prepared using a GST fusion protein containing residues 1622–1690 of KDM5A. Anti-EMSY rabbit polyclonal antibodies were prepared using a GST fusion protein containing a C-terminal EMSY fragment (residues 1013–1313).

Plasmids—cDNAs of human MRG15 (NM_006791), KDM5A (NM_001042603), EMSY (NM_ 020193), and ZMYND8 (isoform a, NM_183047; isoform b, NM_012408; isoform c, 183048) were PCR-amplified from a HeLa cDNA library using the Expand High Fidelity PCR system (Roche Applied Science). The PCR products were cloned into the pCRII vector using the TOPO-TA cloning kit (Invitrogen), sequenced, and then subcloned into each expression plasmid. To obtain Tet-inducible expression plasmids, the KDM5A cDNA was introduced into pcDNA4/TO with a FLAG tag sequence. Other cDNAs were introduced into pCDNA4/TO/3F/puro, a pcDNA4/TO derivative containing the 3×FLAG tag sequences, and the puromycin resistance gene. To express full-length or truncated proteins in HEK293T cells, corresponding cDNAs were introduced into pFLAG-C1 (36). Plasmids were introduced into human cultured cells using the Polyfect transfection reagent (Qiagen) or Lipofectamine 2000 reagent (Invitrogen).

Protein Purification—Affinity purification of MRG15-, KDM5A-, EMSY-, and ZMYND8-containing protein complexes and the LC/MS/MS analyses were performed as described previously (22). Briefly, 10 mg of nuclear extract prepared from T-Rex HeLa cell lines expressing each FLAG-tagged protein was diluted to 2 mg/ml with IP buffer (50 mM HEPES-NaOH (pH 7.9), 0.25–0.3 M NaCl (or KCl), 10% glycerol, 0.2 mM EDTA, 0.1% Triton X-100). The diluted extracts were precleared with Sepharose CL-4B (GE Healthcare) for 1 h at 4 °C and then incubated with anti-FLAG-M2-agarose (Sigma) for 8 h at 4 °C with gentle rotation. The resin was washed sequentially with 3 column volumes of IP buffer containing 0.25 M NaCl/KCl (0.25 M-IP buffer), 2 column volumes of 0.3 M-IP buffer, and 3 column volumes of 0.25 M-IP buffer. Bound proteins were eluted twice with 0.25 M-IP buffer containing 0.25 mg/ml 3×FLAG peptide (Sigma) for 4 h at 4 °C with rotation. The eluates were precipitated with a 2× volume of ethanol, resolved on an 8–16% gradient SDS-polyacrylamide gel (Cosmo Bio), and stained using SilverQuest (Invitrogen). Each specific polypeptide band was excised, destained, and trypsinized for LC-MS/MS analysis. Data from each LC-MS/MS analysis were assembled and analyzed by the proteome software, Scaffold, and the number of assigned spectra and the score obtained from the Mascot Search are summarized in Table 1.

In Vivo Interaction Assay—FLAG-tagged full-length and truncated KDM5A proteins were transiently expressed in HEK293T cells. After 24 h, the cells were harvested, resuspended in IP buffer, and lysed by three freeze-thaw cycles. Cell lysates were clarified by centrifugation at 21,880 × g for 30 min and subjected to immunoprecipitation using anti-FLAG anti-

TABLE 1
Overview of the LC-MS/MS analysis

Protein	Gene ID	No. of peptides (Mascot score)					
		kDa	F-KDM5A IP	F-MRG15 IP	F-EMSY IP	F-ZMIND8 IP
KDM5A	5927	192	674 (6248)	62 (1116)	19 (446)	[a]
MRG15	10,933	37	10 (299)	262 (3776)	13 (308)	
EMSY	56,946	142	38 (486)	96 (703)	88 (1981)	
ZMYND8	23,613	129	27 (431)			155 (1222)
HDAC complex						
SIN3B	23,309	129	17 (412)	35 (616)	21 (475)	
PF1	57,649	110	14 (274)	38 (642)	10 (169)	
GATAD1	57,798	29	3 (80)	6 (178)	2 (172)	
RbAb46/48	5931	48	8 (186)	20 (242)	6 (183)	2 (62)
HDAC1/2	3065	55	10 (106)	18 (253)	6 (102)	1 (52)
CHD4	1108	215	2 (78)			[a]
MTA2	9219	75	11 (337)			4 (122)
GATAD2A	54,815	68	8 (94)			1 (34)
ZNF 592	9640	138	8 (97)			6 (90)
ZNF 687	57,592	130	7 (79)			22 (195)
HAT complex						
TRRAP	8295	438		289 (3266)		
hDomino	57,634	344		182 (2655)		
TIP49A/B	10,856	51	3 (87)	178 (2730)		
BRD8	10,902	103		102 (834)		
DMAP1	55,929	53		39 (632)		
EPC1/2	26,122	86		35 (527)		
TIP60	10,524	56		34 (251)		
BAF53A	86	47		29 (718)		
YL1	6944	42		15 (246)		
ING3	54,556	42		17 (264)		
MRGBP	55,257	22		17 (350)		
GAS41	8089	27		12 (247)		
hEaf6	64,769	21		2 (66)		
H2Av	94,239	12		2 (92)		
H2B	8340	14		2 (77)		
BRCA complex						
PALB2	79,728	131		34 (599)		

[a] Proteins that were not identified by MS analysis but were detected by IP-Western blotting analysis.

bodies. Precipitated proteins were analyzed by Western blotting.

Sucrose Gradient Sedimentation Analysis—KDM5A-interacting proteins were affinity-purified from nuclear extracts (50 mg) prepared from FLAG-KDM5A-expressing cells and loaded on 5–40% sucrose gradients prepared in gradient buffer (25 mM HEPES-NaOH (pH 7.9), 150 mM NaCl, 1 mM EDTA) supplemented with a protease inhibitor mixture (Complete EDTA-free; Roche Applied Science). Centrifugation was performed in a Beckman MLS-50 at 139,000 × *g* for 8 h at 4 °C. Fractions of 200 μl were collected from the top, and aliquots were resolved by SDS-PAGE and analyzed by silver staining or Western blotting.

Tandem Immunoprecipitation—Affinity-purified KDM5A-interacting proteins were divided into 3 aliquots and incubated with rabbit IgG or with anti-SIN3B- or anti-MTA2 antibodies. After a 3-h incubation, the reaction mixtures were further incubated with 50 μl of protein A-agarose beads (Invitrogen) that had been pre-blocked with 0.1% BSA for 1 h. The beads were washed four times with 1 ml of IP buffer. Bound proteins were eluted by boiling in SDS sample buffer and analyzed by Western blotting.

RNA Interference—siRNAs purchased from Cosmo Bio or Sigma were introduced into cells as described previously (37). After 48 h, siRNA-treated cells were harvested and used for Western blotting, qRT-PCR, and ChIP analyses. The siRNAs used in this study were as follows: siKDM5A (mixture), 5′-ccacagaacuaguagaaaaTT-3′; 5′-ggaaauacccagagaaugaTT-3′; 5′-gauaguaguuagaggcuuaTT-3′; siCHD4, 5′-caaacaggagcuugaugauTT-3′; and siSIN3B, 5′-ggucuaagagcuuacucaaTT-3′. A control siRNA mixture was also purchased from Cosmo Bio (catalogue no. C6A-0126).

RNA Isolation and Quantitative Real Time PCR—Total RNA from control and siRNA-treated cells was extracted by TRIzol reagent (Invitrogen). The Power SYBR Green RNA-to-Ct 1-step kit (Applied Biosystems) was used to amplify cDNA fragments, according to the manufacturer's instructions. Real time RT-PCR was carried out using the StepOnePlus Real Time PCR system (Applied Biosystems). All PCRs were performed at least three times.

DNA Microarray Analysis—RNAs prepared from siRNA-treated HeLa cells were analyzed using Whole Human Genome Oligo Microarrays (Agilent Technologies). Labeling and hybridization were performed using the Agilent Gene Expression system according to the manufacturer's instructions (Agilent Technologies). In brief, 100 ng of total RNA was amplified and cyanine 3-CTP-labeled with the One Color Low Input Quick Amp Labeling kit (Agilent Technologies). Labeled cRNA was fragmented and hybridized on the Whole Human Genome Expression Array G4851A (8 × 60K; Agilent Technologies). Images were scanned using a DNA microarray scanner and processed using Feature Extraction software (all from Agilent Technologies). Fluorescence signals were normalized to the 75th percentile. The cutoff value of *t* test for analysis of differential gene expression is ≥1.5-fold change and *p* value <0.05. Gene Ontology analysis and other statistical analyses were conducted using GeneSpring GX (Agilent Technologies). Each microarray experiment was performed two technical replicates. Expression states of several representative genes were confirmed by RT-qPCR analysis with at least three biological replicates. Gene expression data are listed in supplemental Table S1 and can be found in the NCBI's Gene Expression Omnibus (GEO) database through accession number GSE55206.

Chromatin Immunoprecipitation (ChIP)—ChIP was performed as described previously (22). Briefly, siRNA-transfected HeLa cells were fixed with 1% formaldehyde for 5–10 min at room temperature. The cell suspension in SDS lysis buffer (50 mM Tris-HCl (pH 8.0), 1% SDS, 10 mM EDTA) was transferred to TPX microtube (Diagnode) and sonicated with a Bioruptor (Cosmo Bio) (level High, 30 s/30 s-ON/OFF, 10 cycles). The sonicated samples were diluted with ChIP dilution buffer (16.7 mM Tris-HCl (pH 8.0), 167 mM NaCl, 0.01% SDS, 1.1% Triton X-100, 1.2 mM EDTA) and immunoprecipitated with antibody-conjugated Dynabeads (sheep anti-mouse IgG, Invitrogen) at 4 °C overnight. The beads were then washed sequentially with low salt buffer (20 mM Tris-HCl (pH 8.0), 150 mM NaCl, 0.1% SDS, 1% Triton X-100, 2 mM EDTA), high salt buffer (20 mM Tris-HCl (pH 8.0), 500 mM NaCl, 0.1% SDS, 1% Triton X-100, 2 mM EDTA), LiCl buffer (10 mM Tris-HCl (pH 8.0), 0.25 M LiCl, 1% Nonidet P-40, 1% sodium deoxycholate, 1 mM EDTA), and TE buffer. The protein-DNA complexes were eluted with Elution buffer (10 mM Tris-HCl (pH 8.0), 300 mM NaCl, 0.5% SDS, 5 mM EDTA) and decross-linked for 6 h at 65 °C. The immunoprecipitated DNA was recovered by phenol/chloroform extraction and ethanol precipitation after proteinase K treatment. ChIPed DNA was analyzed with the StepOnePlus Real Time PCR system (Applied Biosystems). For sample amplification, the Fast SYBR Green Master Mix (Applied Biosystems) was used. All PCRs were performed at least three times.

Nematode Strains and Culture Conditions—N2 Bristol was used as the wild-type strain (38). Animals were cultured at 15 °C for maintenance and at 22 or 24 °C for analyzing the vulvaless and multivulva (Muv) phenotypes at the L4 stage. The mutants used in this study were *rbr-2*(*tm1231*) and *let-418*(*n3536*).

RESULTS

KDM5A Associates with Two HDAC Complexes—We previously identified KDM5A during a proteomic analysis of MRG15-associated proteins (Fig. 1*A* and Table 1) and demonstrated functional association between KDM5A and the SIN3B-HDAC complex (22). Given KDM5A's involvement in diverse biological processes, we were interested in characterizing KDM5A-associated protein interaction networks. HeLa cell lines expressing tetracycline-inducible, N-terminal FLAG-tagged KDM5A (F-KDM5A) were produced, and F-KDM5A-associated proteins were purified from HeLa nuclear extracts using anti-FLAG affinity gel chromatography. Mass spectrometry (MS) analysis of the purified fraction detected most of the previously identified MRG15-associated proteins, including components of the SIN3B-HDAC complex (SIN3B complex) (Fig. 1*B* and Table 1, F-KDM5A-IP). In both F-MRG15 and F-KDM5A affinity-purified fractions, we identified a novel protein, EMSY, which was originally identified as a BRCA2-interacting protein (39), and was not clearly identified in our previous study (22). Of note, F-KDM5A was also copurified with additional proteins, including CHD4, MTA2, GATAD2A, ZMYND8A, ZNF592, and ZNF687 (Fig. 1*B* and Table 1). Among these, CHD4, MTA2, and GATAD2A are known components of the NuRD complex (28). The presence of these proteins in the F-KDM5A-purified fractions was further confirmed by Western blot analysis (Fig. 1*E*). These findings demonstrated the physical association between KDM5A and NuRD complex components.

To further characterize the KDM5A-interacting proteins, a similar affinity purification was conducted for the two previously uncharacterized factors, EMSY and ZMYND8A, and the interacting proteins were analyzed by mass spectrometry. EMSY was associated with KDM5A and SIN3B complex components, although no association was observed with NuRD complex components (Fig. 1, *C* and *F*, and Table 1). In contrast, ZMYND8A was stably associated with NuRD complex components (MTA2 and GATAD2A), ZNF592, and ZNF687 but not with MRG15 or other SIN3B complex components (Fig. 1, *D* and *G*, and Table 1). Although ZMYND8A was clearly identified in the F-KDM5A-purified fraction (Fig. 1, *B* and *E*, and Table 1), peptides for KDM5A were not detected in ZMYND8A-purified fractions (Fig. 1*D* and Table 1). Because interactions between KDM5A and three ZMYND8 isoforms were clearly detected by Western blot analysis (Fig. 1*H*), it is likely that a minor population of ZMYND8 interacts with KDM5A-associated complexes.

Taken together, these results suggested that KDM5A physically associates with two distinct SIN3B and NuRD complexes. Our results also showed that EMSY is a specific component of the SIN3B complex, consistent with a previous proteomic analysis using *Drosophila* embryos (26). Although ZMYND8, ZNF592, and ZNF687 were recently identified as forming the Z3 coregulator complex, which associates with several histone demethylase machineries (40), our results suggested that ZMYND8, ZNF592, and ZNF687 preferentially associate with the NuRD complex.

Characterization of KDM5A-interacting Factors—To further characterize the F-KDM5A-associated proteins, the F-KDM5A-purified fraction was subjected to sucrose density gradient centrifugation. Although KDM5A was primarily detected in fractions corresponding to its molecular mass (~193 kDa), it was also detected in fractions corresponding to more than 600 kDa (Fig. 2*A*, *fractions 11–19*). This analysis also revealed that most of the minor bands detected below F-KDM5A in polyacrylamide gels were its degraded species, presumably cleaved by endogenous proteinases (Fig. 2*A*, *αFLAG*). Importantly, the SIN3B complex-specific components, SIN3B, MRG15, and PF1, migrated slightly slower than the NuRD complex-specific components, MTA2 and GATAD2A, and the migration profile of KDM5A largely overlapped with those of the SIN3B and NuRD complex components. In addition, a shared component, HDAC2, was broadly distributed in fractions that overlapped with each of the complex-specific components. This analysis supported our affinity purification results showing that KDM5A is physically associated with both the SIN3B and NuRD complexes.

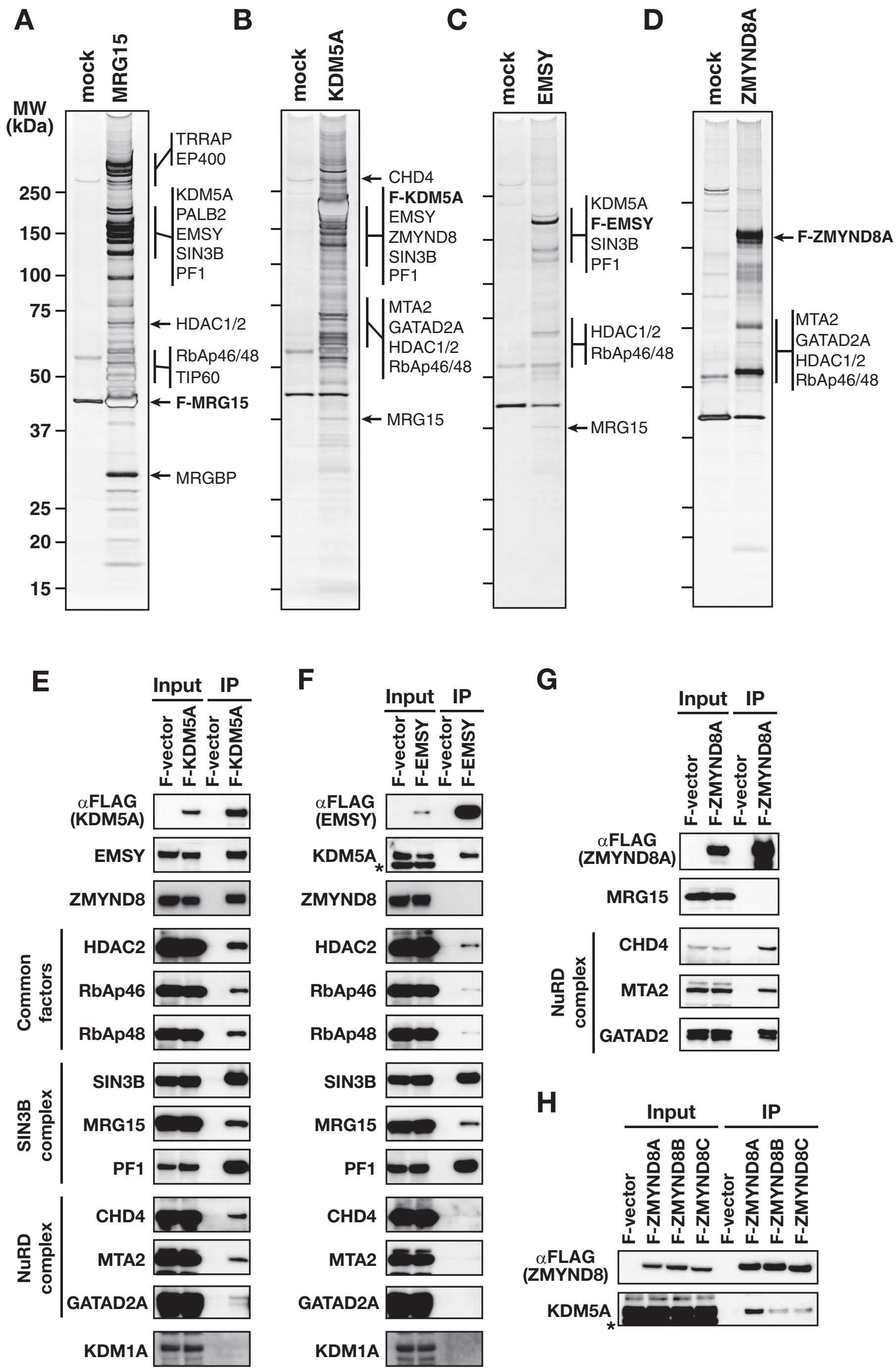

FIGURE 1. **KDM5A is associated with two distinct HDAC complexes.** *A,* immunopurified FLAG-tagged MRG15-containing complexes resolved by SDS-PAGE and analyzed by silver staining. A mock purification from cells containing the empty expression vector, with the FLAG epitope tag, is shown as a control (*mock*). Proteins identified by LC-MS/MS analysis are indicated at *right*. *B–D,* immunopurified FLAG-KDM5A-containing (*B*), FLAG-EMSY-containing (*C*), or FLAG-ZMYND8A-containing (*D*) complexes resolved and analyzed as in *A*. Detailed LC-MS/MS results are provided in Table 1. *E–G,* whole cell lysates (*Input*) of HeLa cells expressing FLAG-tagged KDM5A (*E*), EMSY (*F*), or ZMYND8A (*G*) and anti-FLAG immunoprecipitates (*IP*) were subjected to immunoblotting using the indicated antibodies. *H,* whole cell lysates (*Input*) of HeLa cells expressing FLAG-tagged ZMYND8A, ZMYND8B, or ZMYND8C, and anti-FLAG IPs subjected to immunoblotting using the anti-KDM5A antibody. Factors previously identified in both SIN3B and NuRD complexes (common factors), specifically in the SIN3B complex (SIN3B complex) or specifically in the NuRD complex (NuRD complex), are indicated at *left*. *Asterisks* indicate nonspecific protein bands.

To confirm that KDM5A associates with two distinct HDAC complexes, a two-step purification analysis was performed. Affinity-purified F-KDM5A-interacting proteins (Fig. 1*B*) were further immunoprecipitated with either anti-SIN3B or anti-MTA2 antibodies. Western blot analysis revealed that SIN3B IPs contained MRG15 and EMSY but not MTA2 or ZMYND8 (Fig. 2*B*), whereas MTA2 IPs contained ZMYND8 but not SIN3B, MRG15, or EMSY. F-KDM5A was detected in both SIN3B and MTA2 IPs. These results clearly support our conclusion that KDM5A is physically associated with two distinct complexes, SIN3B and NuRD.

KDM5A Uses Distinct Domains to Associate with the SIN3B and NuRD Complexes—To dissect the molecular basis for KDM5A's interactions with the two HDAC complexes, we per-

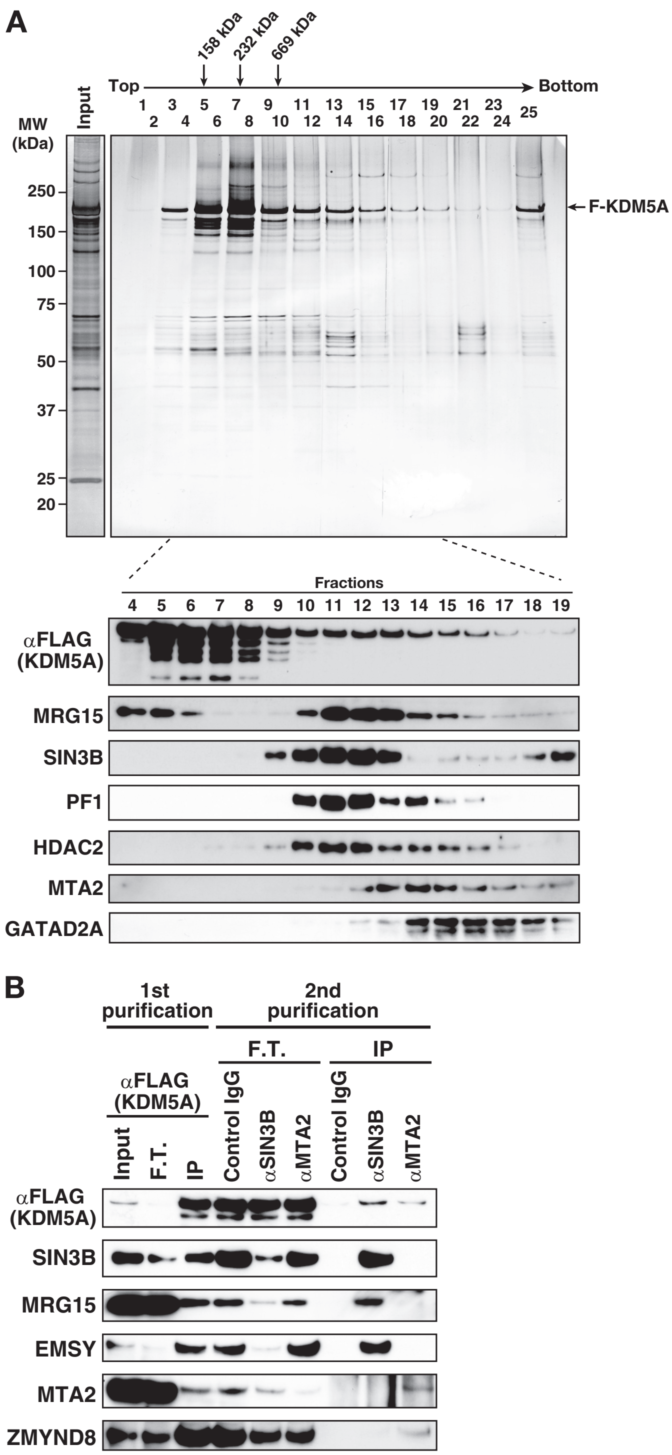

FIGURE 2. **Characterization of KDM5A-interacting factors.** *A*, affinity-purified KDM5A-associating proteins (*Input*) were subjected to a sucrose gradient sedimentation analysis. Proteins in collected fractions were subjected to SDS-PAGE and analyzed by silver-staining or immunoblotting using the indicated antibodies. Aldolase (158 kDa), catalase (232 kDa), and thyroglobulin (669 kDa) were used as molecular mass standards. *B,* tandem immunoprecipitation analysis. Affinity-purified KDM5A-interacting proteins were immunoprecipitated using anti-SIN3B or anti-MTA2 antibodies, and the precipitated proteins were immunoblotted using the indicated antibodies. *F.T.* means flow-through fractions.

formed a structure-function analysis of KDM5A. A series of FLAG-tagged truncated KDM5A proteins were transiently expressed in HEK293T cells and assessed for their ability to bind MRG15 (SIN3-HDAC-specific component) or ZMYND8 (NuRD-specific component) (Fig. 3). As summarized in Fig. 3*D*, N-terminally truncated KDM5A polypeptides completely lost their ability to bind MRG15 (Fig. 3*A*). KDM5A deletion proteins containing residues 1–798 bound to MRG15, but more extensive C-terminal deletion proteins did not (Fig. 3*B*), suggesting that the N-terminal region spanning residues 1–798 mediates interaction with the SIN3B complex. In contrast, none of C-terminal deletion proteins could bind ZMYND8 (Fig. 3*C*), and the N-terminal truncation in which the JmjC domain was deleted was also unable to bind ZMYND8 (Fig. 3*C*), suggesting that KDM5A's interaction with the NuRD complex is mediated by a region that spans the JmjC domain to the C terminus (residues 437–1690) (Fig. 3*D*). These results suggested that KDM5A uses distinct domains to bind to the SIN3B-HDAC and NuRD complexes.

Comparison of Genes Regulated by KDM5A, SIN3B, or CHD4—To investigate the functional associations between KDM5A and the two HDAC complexes, we first examined the expression levels of three KDM5 family proteins, KDM5A, KDM5B, and KDM5C, in several tumor cell lines. Because all of these cell lines were derived from female cells, the other family member, KDM5D, which is encoded by a gene on the Y chromosome, was not expressed in these cells.

KDM5A mRNA was predominantly expressed in HeLa and U2OS cells, although the expression levels of the other two family members were relatively higher in 293T and MCF7 cells (Fig. 4*A*). Western blot analysis revealed similar relative protein levels (Fig. 4*B*). Considering that the physical association between KDM5A and the NuRD complex was detected in HeLa cells (Fig. 1) and that *KDM5A* was predominantly expressed in HeLa cells (Fig. 4, *A* and *B*), we decided to use this cell line to investigate the functional association between KDM5A and the NuRD complex.

We performed siRNA-mediated knockdown of KDM5A, CHD4, or SIN3B in HeLa cells (Fig. 4*C*) and analyzed the changes in gene expression by microarray analysis (Fig. 4*D* and supplemental Table S1). At least 435 genes (corresponding to 468 probes) were dysregulated in the KDM5A-knockdown cells (fold change $\geq$1.5 and p value $<$ 0.05). Notably, 66 and 63% of the KDM5A-regulated genes were also dysregulated in CHD4- and SIN3B-knockdown cells, respectively (Fig. 4*D*), and 47% of the KDM5A-regulated genes were affected by either CHD4 or SIN3B knockdown.

Heat map representation indicated that among the 435 KDM5A-regulated genes, 40% were up-regulated, although more than half were down-regulated (Fig. 4*E*). Interestingly, a similar proportion of genes was down-regulated in response to SIN3B knockdown (Fig. 4*E*). Gene ontology analysis of the genes that were commonly regulated by KDM5A and CHD4 revealed that genes associated with developmental processes were the most significantly regulated (Fig. 4*F*), whereas the genes commonly regulated by KDM5A and SIN3B were not associated with any particular biological processes (data not shown).

Characterization of Genes Commonly Regulated by KDM5A and CHD4—Although 66% of the KDM5A-regulated genes were also changed by CHD4 knockdown, the change was not

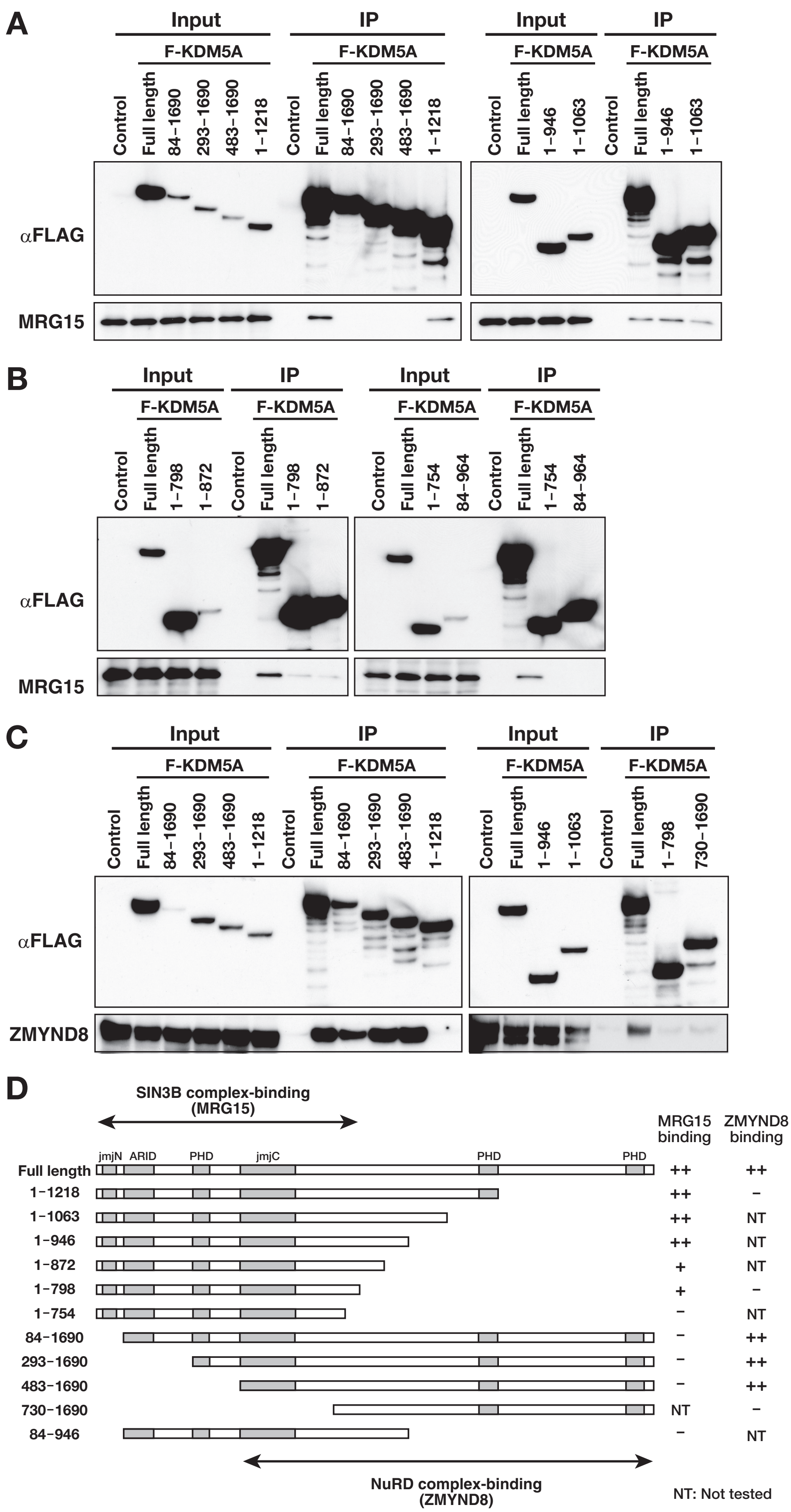
A
Input
IP
F-KDM5A
Control
Full length
84–1690
293–1690
483–1690
1–1218
1–946
1–1063
αFLAG
MRG15
B
1–798
1–872
1–754
84–964
C
730–1690
ZMYND8
D
SIN3B complex-binding
(MRG15)
jmjN
ARID
PHD
jmjC
MRG15 binding
ZMYND8 binding
Full length ++ ++
1–1218 ++ –
1–1063 ++ NT
1–946 ++ NT
1–872 + NT
1–798 + –
1–754 – NT
84–1690 – ++
293–1690 – ++
483–1690 – ++
730–1690 NT –
84–946 – NT
NuRD complex-binding
(ZMYND8)
NT: Not tested

necessarily in the same direction. We divided these 309 genes into four categories according to the knockdown effect (Fig. 5*A*), and the altered expression of representative genes in each category was confirmed by quantitative RT-PCR analysis (Fig. 5*B*). The expression of selected genes was either up-regulated or down-regulated by KDM5A or CHD4 knockdown in a manner consistent with the microarray data (supplemental Table S1). To corroborate the functional link between KDM5A and CHD4, we simultaneously depleted these proteins and analyzed the changes in gene expression. The double knockdown of KDM5A and CHD4 showed, at most, limited additivity (Fig. 5*B*). Because the knockdown efficiencies were generally comparable in the single- and double-knockdown experiments (Fig. 5*B*, *KDM5A* and *CHD4*), we consider it unlikely that incomplete knockdown limited the amount of additivity. Rather, these results suggested that, at least for a subset of genes, KDM5A and CHD4 function in the same pathway. In addition, for the genes in categories I, II, and IV, the effect of the double knockdown was almost the same as that of KDM5A single knockdown, indicating that KDM5A may have a dominant role in regulating the expression of these genes.

To further characterize the functional association between KDM5A and CHD4, we examined the effect of depleting these factors in other cell lines (Fig. 5, *C–E*). Although the expression pattern of KDM5 family proteins in U2OS cells was similar to that in HeLa cells, the effect of KDM5A or CHD4 knockdown was different between these two cell lines. In addition, the expression levels of some genes were not markedly changed in 293T or MCF7 cells after KDM5A or CHD4 knockdown. These results suggested that KDM5A targets some genes in a cell type-specific manner and/or that KDM5A may function cooperatively with other KDM5 family proteins to control the target genes in other cell types.

KDM5A and the NuRD Complex Cooperatively Regulate H3K4me2/3 Levels—To further explore the functional association between KDM5A and the NuRD complex, we performed ChIP assays and examined the H3K4 methylation levels at the transcriptional start sites (TSSs), gene bodies (GBs), and transcriptional termination sites (TTSs) of the candidate target genes in each category (Fig. 6*A*).

These ChIP analyses showed that H3K4me3 was modestly enriched at the TSS and gene body of the genes in category I (Fig. 6*A*, *GDF15* and *KLF2*). Depletion of KDM5A or CHD4 caused an increase in H3K4me3 at the examined genomic regions. Again, double knockdown of KDM5A and CHD4 showed limited additivity. These results suggested that both KDM5A and CHD4 function in controlling the H3K4me3 levels of these genes.

Although relatively high H3K4me3 levels were detected at some genomic regions of genes in other categories, such as *HES7* or *PDGFA*, the H3K4me3 levels at some other candidate target genes were very low, and the knockdown of KDM5A showed little impact on the H3K4me3 levels at the examined genomic regions. Although these genes in categories II, III, and IV emerged as candidate targets for KDM5A in the expression analysis (Fig. 4), it is likely that KDM5A knockdown indirectly affected their expressions.

To further investigate the functional association between KDM5A and CHD4, we examined the H3K4me2 and H3K36me3 levels, as well as the chromatin associations of KDM5A and CHD4, at the genomic loci of the candidate target genes in category I. Although both H3K4me2 and H3K36me3 were broadly present throughout the transcribed regions of *GDF15*, they showed a distinct distribution pattern at the genomic regions of *KLF2*; H3K4me2 was decreased at the transcriptional termination sites, and H3K36me3 was increased from the gene body to the transcriptional termination sites (Fig. 6, *B* and *C*). The knockdown of KDM5A or CHD4 caused a slight increase in H3K4me2, but it had little impact on the H3K36me3 levels at the examined regions. Taken together, these results suggested that the transcriptional changes caused by KDM5A- or CHD4-knockdown were primarily correlated with increased H3K4me2/3 levels.

Our ChIP analysis also showed that KDM5A and CHD4 were broadly localized to the examined genomic regions (Fig. 6, *E* and *F*). Interestingly, CHD4's localization to these regions was partially impaired by KDM5A knockdown (Fig. 6*F*), whereas KDM5A's localization was not markedly changed by CHD4 knockdown (Fig. 6*E*). These results suggested that KDM5A promotes CHD4's chromatin association.

It has been unclear how CHD4, which belongs to the ATP-dependent chromatin remodeling factors, regulates H3K4me2/3 levels. In this regard, our ChIP analysis showed slight differences in the amount of whole H3 enrichment with CHD4 knockdown among the examined genomic regions (Fig. 6*D*). Although the biological relevance of this result needs to be clarified, the differences in H3 enrichment may reflect changes in the nucleosomal occupancy or dynamics at these genomic regions, which could modulate the action of KDM5A and/or other counteracting H3K4-specific methyltransferases.

KDM5A C. elegans Homologue RBR-2 Functions Cooperatively with NuRD in Vulval Development—Although mammals have four KDM5 family members and we cannot exclude the possibility of their overlapping function, other organisms such as *Drosophila* and *C. elegans* have only one KDM5 homologue. To obtain further evidence for a functional interaction between KDM5 and the NuRD complex during developmental processes, we examined the role of RBR-2 in *C. elegans* vulval development (Fig. 7*A*).

In *C. elegans*, the specification of the vulval cell fate is antagonized by the synthetic multivulva (synMuv) genes (41). The synMuv genes are grouped into three classes (A, B, and C) on the basis of genetic interactions (42). Animals homozygous for loss-of-function mutations in any two synMuv gene classes give

FIGURE 3. **KDM5A uses distinct domains to associate with the SIN3B and NuRD complexes.** *A–C,* whole cell lysates (*Input*) of HEK293T cells expressing FLAG-tagged full-length or truncated KDM5A proteins, and anti-FLAG IPs were immunoblotted using the indicated antibodies. *D,* summary of the domain analysis. Schematic drawing of the full-length and truncated FLAG-KDM5A constructs tested in the binding assay are shown at *left*. *Gray boxes* indicate the conserved domains found in KDM5 family proteins. KDM5A regions required for binding to the SIN3B (MRG15) and NuRD (ZMYND8A) complexes are indicated at the top and bottom, respectively. ++, strong binding; +, weak binding; −, not bound; *NT,* not tested.

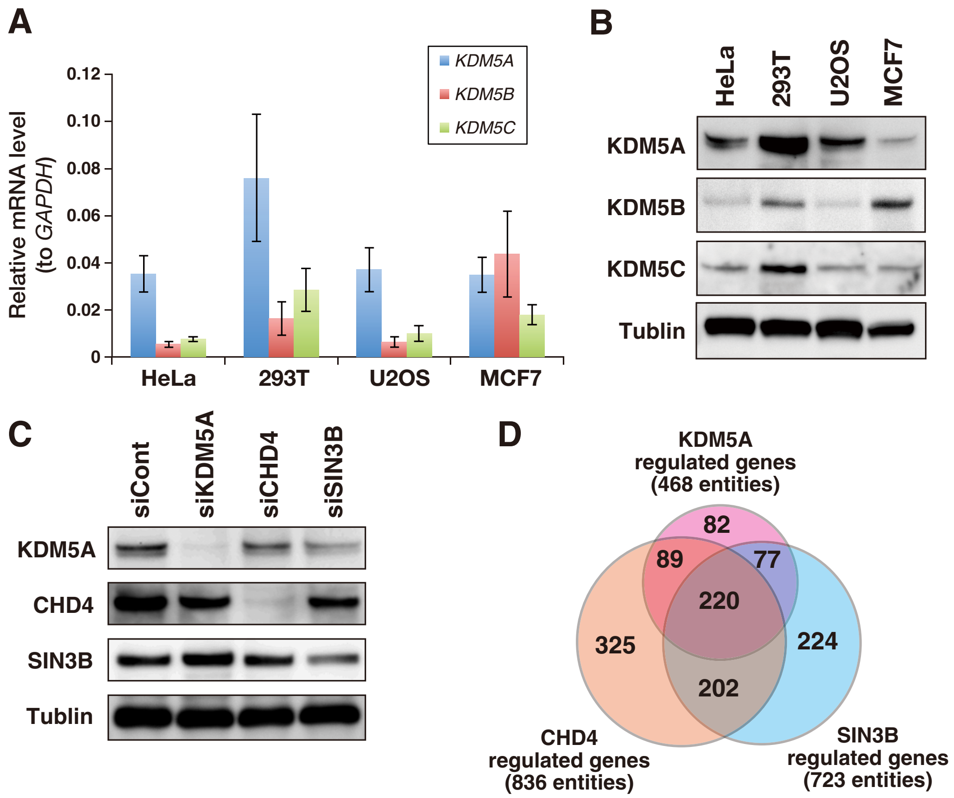

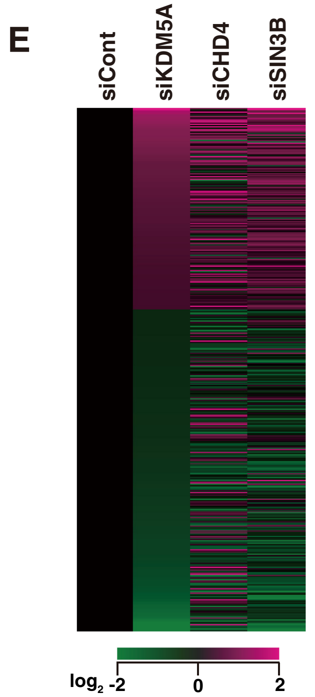

F

GO Term	*P*-value
System Development	6.22e-09
Anatomical Structure Development	4.00e-09
Epidermis Development	4.90e-08
Tissue Development	1.21e-07
Developmental Process	2.04e-07
Response to Extracellular Stimulus	2.14e-07
Multicellular Organismal Development	3.13e-07
Response to External Stimulus	1.47e-06
Multicellular Organismal Process	1.94e-06
Response to Nutrient Levels	2.48e-06
Regulation of Cell Migration	5.05e-06
Response to Steroid Hormone Stimulus	4.62e-06
Positive Regulation of Cell Adhesion	4.98e-06
Organ Development	6.19e-06
Regulation of Cell Motility	6.06e-06
Platelet-derived Growth Factor Receptor Binding	7.62e-06
Response to Chemical Stimulus	8.00E-06
Response to Drug	1.19E-05
Regulation of Smooth Muscle Cell Migration	1.13E-05
Regulation of Cellular Component Movement	1.75E-05

FIGURE 4. **Comparison of genes regulated by KDM5A, SIN3B, or CHD4.** *A* and *B*, expression levels of three KDM5 family genes in HeLa, HEK293T, U2OS, or MCF7 cells. The levels were determined by quantitative real time-PCR (qRT-PCR) (*A*) and immunoblotting using the indicated antibodies (*B*). The RT-PCR values were normalized to the *GAPDH* level. *Error bars* represent standard deviations of three biological replicates. *C*, HeLa cells were treated with the control (*siCont*) or indicated siRNAs, and the levels of endogenous KDM5A, CHD4, SIN3B, or tubulin (loading control) were analyzed by Western blotting. *D*, Venn diagram representing the genes dysregulated by KDM5A-, CHD4-, or SIN3B-knockdown in HeLa cells. Genes displaying ≥1.5-fold changed expression and a p value < 0.05 were included in the dataset. *E*, heatmap representation of genes regulated by KDM5A, CHD4, or SIN3B. Genes commonly regulated by KDM5A, CHD4, and SIN3B were sorted according to the level of change induced by KDM5A-knockdown. *Shades* of *green* and *magenta* indicate down-regulation and up-regulation, respectively. *F*, gene ontology (*GO*) analysis of genes commonly regulated by KDM5A and CHD4.

rise to a Muv phenotype resulting from abnormal vulval precursor cells induction, whereas animals homozygous for loss-of-function mutations in any single synMuv gene class do not exhibit the Muv phenotype. Genes encoding homologues of mammalian NuRD complex components such as LET-418 (CHD4), LIN-53 (RbAp46/48), and HAD-1

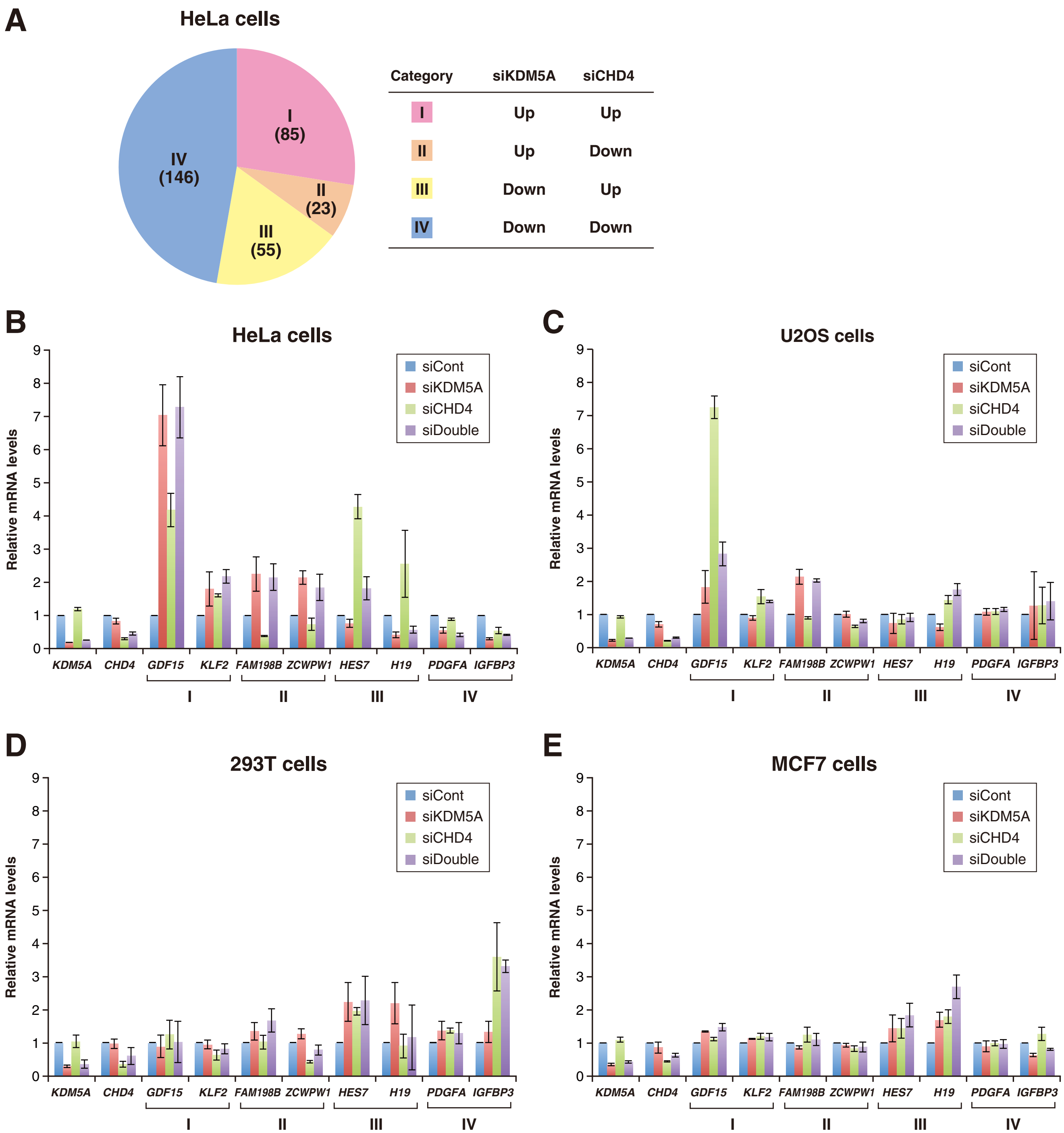

FIGURE 5. **Validation of genes regulated by KDM5A and NuRD.** *A*, categorization of the genes that were dysregulated in both siKDM5A- and siCHD4-treated cells. The genes were classified into four categories according to the effect of each siRNA treatment. *B–E*, expression levels of representative genes of each category in siRNA-treated HeLa (*B*), U2OS (*C*), HEK293T (*D*), and MCF7 (*E*) cells. The levels were determined by qRT-PCR after each knockdown and were compared with the levels of control siRNA-treated cells. The values were normalized to *GAPDH* levels. *Error bars* represent standard deviations of three biological replicates.

(HDAC1), genetically interact with synMuvA genes to generate the Muv phenotype and are categorized as the class B synMuv genes (42).

A previous report showed that the *rbr-2*(*tm1231*) mutant exhibits complex defects in vulval development, leading to distinct populations of *C. elegans* exhibiting either the Muv or a vulvaless phenotype (17). To investigate the detailed role of RBR-2 in vulval development, we first confirmed that the *rbr-2*(*tm1231*) mutant displayed the Muv (Fig. 7*B*) or vulvaless (Fig. 7*C*) phenotype. The penetrance of the Muv phenotype at 20 °C (25%) (Fig. 7*D*) was higher than previously reported (12.5%), and the penetrance for the undeveloped vulva phenotype (vulvaless) (1%) was considerably lower than previously observed (70%). The differences in penetrance could be due in part to differences in growth conditions (15 and 20 °C), because vulval development and the penetrance of the Muv phenotype are

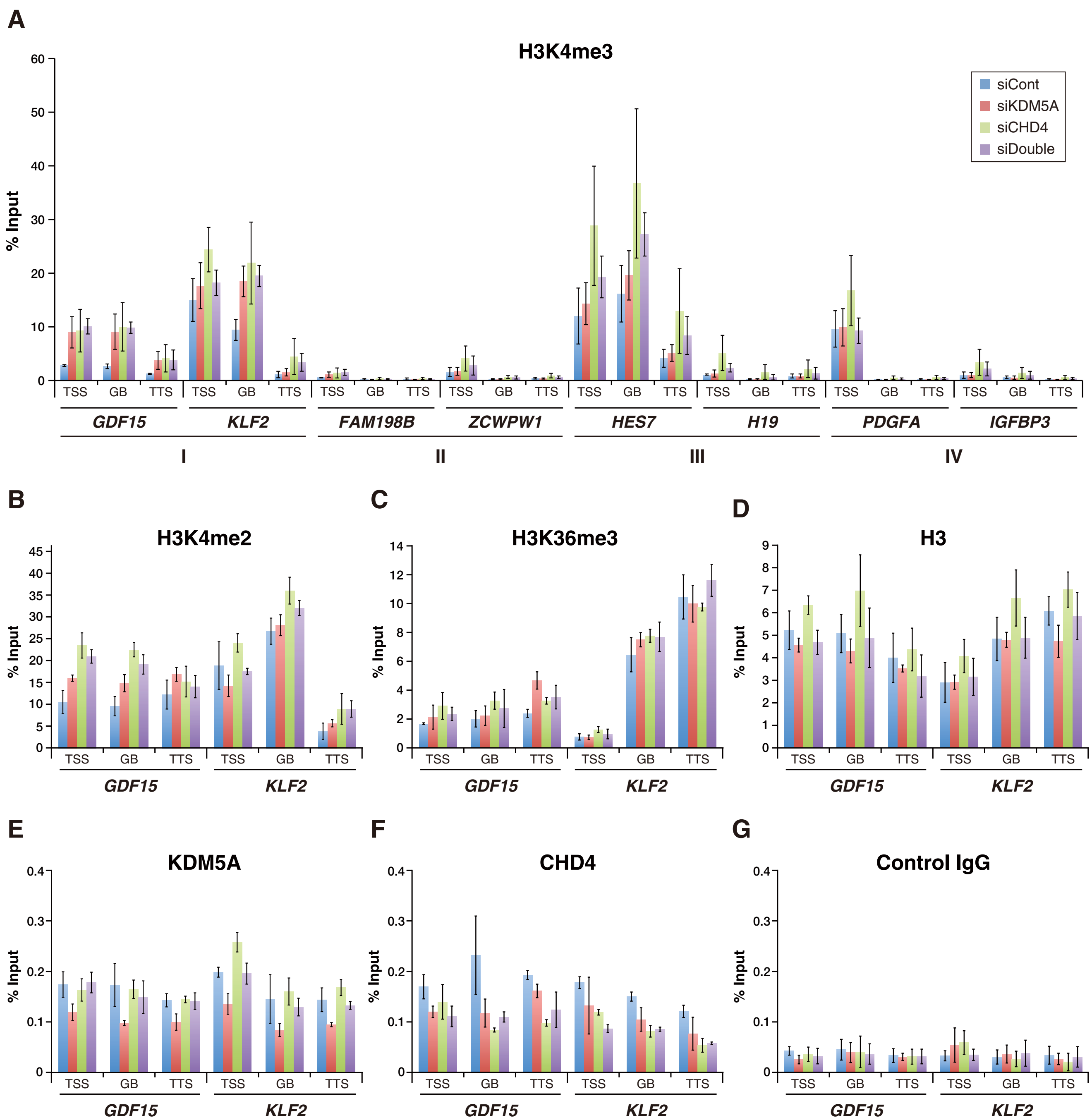

FIGURE 6. **KDM5A and the NuRD complex regulate the H3K4me2/3 levels at representative genes.** *A–G*, results of the ChIP analysis monitoring the distribution of K4-trimethylated H3 (H3K4me3) (*A*), H3K4me2 (*B*), H3K36me3 (*C*), whole histone H3 (*D*), KDM5A (*E*), and CHD4 (*F*), after treatment with each siRNA. The results of ChIP analysis using control IgG are also shown (*G*). Primers were constructed targeting the TSS, the gene body (*GB*), and the transcriptional termination site (*TTS*) of each gene. The level of enrichment in the ChIP was analyzed by qRT-PCR. Values represent the ratio of precipitated DNA to input DNA (%). *Error bars* represent standard deviations of three biological replicates.

affected by the culturing temperature. Regardless of the varied penetrance, the Muv phenotype of the *rbr-2* mutant suggested that *rbr-2* negatively controls vulval development and does not simply function as a synMuvA or synMuvB gene.

Although *let-418* is classified as a synMuvB gene and shows genetic interaction with synMuvA genes (42), the temperature-sensitive *let-418*(*n3536*) mutant was found to display the Muv phenotype at 24 °C (Fig. 7, *D* and *E*) (43). This result suggested that *let-418* does not simply function as a synMuvB gene but may genetically interact with both synMuvA and synMuvB genes, consistent with results of a previous study using RNAi (44). We also noticed that the Muv penetrance of *let-418*(*n3536*) at 24 °C was comparable with that of *rbr-2*(*tm1231*) (Fig. 7, *D* and *E*). To examine genetic interactions between *rbr-2* and *let-418*, we generated mutant strains harboring both *rbr-2*(*tm1231*) and *let-418*(*n3536*) alleles and analyzed vulval development at the restrictive temperature (24 °C). Interestingly, no obvious additive effect was observed in the *rbr-2*(*tm1231*) *let-418*(*n3536*) double mutants compared with each single mutant phenotype (Fig. 7, *D* and *E*). Taken together, these results

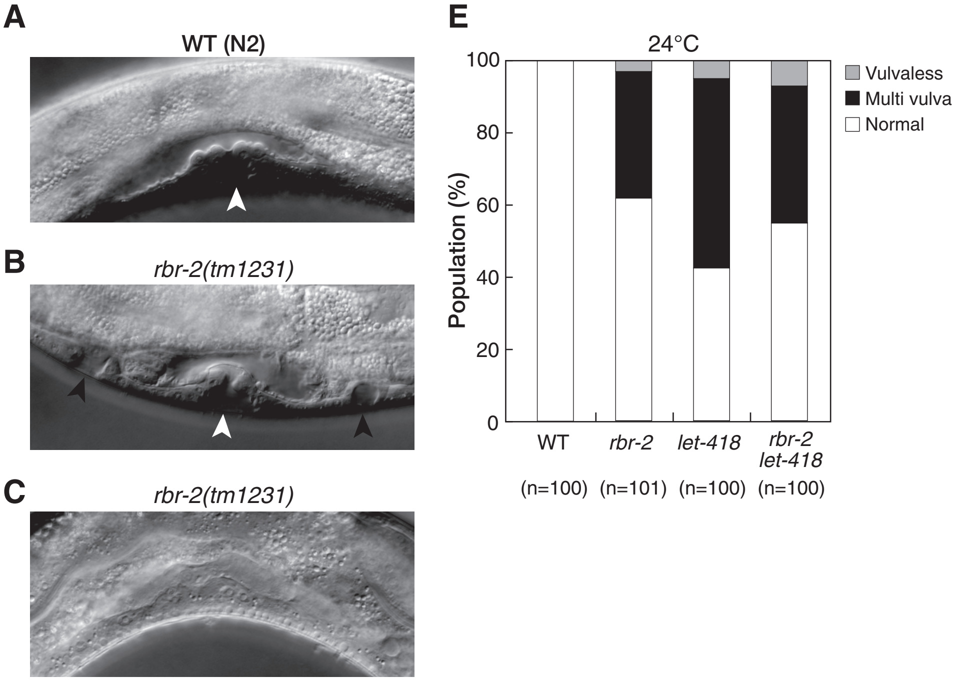

D

Genotype	20°C			22°C			24°C		
	% wt	% muv	% vul	% wt	% muv	% vul	% wt	% muv	% vul
WT (N2)	100	0	0	100	0	0	100	0	0
rbr-2(tm1231)	74	25	1	67	31	2	62	35	3
let418(n3536)	100	0	0	100	0	0	43	53	5
rbr-2(tm1231); let418(n3536)	68	27	5	67	29	4	55	38	7

FIGURE 7. **KDM5A *C. elegans* homolog RBR-2 functions cooperatively with NuRD in vulval development.** *A–C,* differential interference contrast microscopic images of a developing vulva in WT (N2) (*A*) and the *rbr-2*(*tm1231*) mutant (*B* and *C*). *White arrowheads* indicate the vulval invagination, and *black arrowheads* indicate extra-invaginations. A vulvaless mutant animal is also shown (*C*). *D, table* depicting the percentage of animals exhibiting normal vulva (*wt*), multivulva (*muv*), or vulvaless (*vul*) phenotypes. Animals were cultured at 15 °C for maintenance and at 20, 22, or 24 °C to analyze muv and vul phenotypes at the L4 stage. *E,* percentage of animals showing multivulva and vulvaless phenotypes at the restricted temperature (24 °C) (*D*) shown in a graphic representation.

strongly suggested that RBR-2/KDM5 and LET-418/CHD4 function in the same pathway and that both negatively regulate vulval development.

DISCUSSION

We report a biochemical characterization of KDM5A that reveals a novel interaction between KDM5A and the NuRD complex. We further demonstrated that KDM5A and the NuRD complex cooperatively function to control H3K4me3 levels associated with target genes. Our findings demonstrate the conserved interplay between histone demethylation and ATP-dependent chromatin remodeling.

Functional interaction between histone-modifying enzymes and the chromatin-remodeling complex is critical for coordinated gene expression. Although this study revealed physical and functional interactions between KDM5A and the NuRD complex, another KDM5 family protein, KDM5B/JARID1B, has also been shown to interact with the NuRD complex (45). Together, these results suggest that the functions of KDM5 family demethylases are closely linked to the chromatin remodeling activities exhibited by the NuRD complex. In the previous study, however, no physical association between KDM5B and the SIN3B HDAC complex was detected. In addition, although the expression level of endogenous *KDM5B* is lower than that of *KDM5A* in HeLa cells, we could not detect any KDM5B peptides in the MRG15-containing SIN3B complex (Fig. 1), indicating that the ability to interact with both SIN3B HDAC and NuRD complexes may be KDM5A-specific.

In mammals, there are four KDM5 family members, and their demethylase activities have all been demonstrated. However, the functional interactions of each of these KDM5 family members remain unclear. KDM5A is ubiquitously expressed, whereas KDM5B has a restricted expression pattern in normal human adult tissues, with up-regulated expression observed in breast cancer (46). Recent studies also showed an important role for KDM5B in cellular differentiation and development (13, 47). Considering that KDM5 family members share functional domains besides the JmjC domain, we favor the view that KDM5B, KDM5C, and KDM5D target specific genes to establish a repressed state during early development and that KDM5A maintains the repressed states in the subsequent cellular lineages together with the SIN3B HDAC and NuRD complexes. Consistent with this scenario, impaired expression patterns of the KDM5 family members may contribute to tumorigenesis and cancer progression (6 – 8).

KDM1A/LSD1 is an amine oxidase-type demethylase for H3K4 and a stable component of the NuRD complex (48).

KDM1A was also identified as a KDM5B-associated factor (45). In our biochemical studies, however, KDM1A was not detected in the purified KDM5A fraction (Fig. 1, *B* and *E*). Therefore, the functional interaction between KDM5A and KDM1A is unclear. Although no physical interaction was detected in our study, KDM1A was shown to be associated with the NuRD complex at active enhancers in mouse embryonic stem cells (49). Therefore, it is possible that KDM1A and KDM5A associate with the NuRD complex in a chromatin context-dependent manner. Another study showed that KDM5A physically interacts with the H3K9 methyltransferase G9a in murine erythroid cells and functions cooperatively to repress embryonic β-globin gene expression (50). Although neither G9a nor its partner GLP was detected in our KDM5A complexes (Fig. 1*B* and Table 1), it is conceivable that KDM5A interacts with distinct partners during different stages of development.

Using *C. elegans* as a model system, we found that RBR-2/KDM5 and LET-418/CHD4 functioned in the same pathway to negatively regulate vulval development. A previous study showed that animals carrying a mutation in *let-418*(*ar114*) display a highly penetrant synMuv phenotype when it is combined with a synMuvA mutation (51). However, another report showed that *let-418(RNAi)* produces a significant percentage of Muv-positive animals in both synMuvA and synMuvB mutant backgrounds (44). Because animals carrying the temperature-sensitive *let-418* allele (*n3536*) displayed the Muv phenotype at the restricted temperature (Fig. 7*D*) (43), it is likely that the LET-418/CHD4 function is associated with both synMuvA and synMuvB pathways. Although we showed that RBR-2/KDM5 and LET-418/CHD4 functioned in the same pathway during vulval development (Fig. 7, *D* and *E*), *let-418* mutants displayed a more severe developmental defect than the *rbr-2* mutant (51), indicating that the NuRD complex may play a more fundamental role than RBR-2 in development. The detailed molecular mechanisms linking the RBR-2/KDM5 and LET-418/CHD4 functions to vulval development are currently unclear. It has been proposed that the synMuv genes function within the hypodermal hyp7 syncytium to repress ectopic expression of the vulval precursor cell inducer LIN-3 (42). The multivulva phenotype suggests that RBR-2/KDM5 and LET-418/CHD4 may function cooperatively to repress *lin-3* expression in hyp7 cells. Given that many synMuv genes are broadly expressed throughout development, it is conceivable that RBR-2 plays an important role in other developmental processes in collaboration with the NuRD complex.

Although our study demonstrates cross-talk among histone demethylase, histone deacetylase, and histone remodeling activities, the mechanism by which these enzymatic activities are integrated on the chromatin of target genes remains unclear. In addition to the JmjC domain, responsible for histone H3K4 demethylase activity, KDM5A possesses two functional modules, the PHD fingers and the ARID domain. One PHD finger of KDM5A has been shown to recognize H3K4me3 and to play a critical role in leukemia when fused with other proteins such as nucleoporin 98 (52). In addition, the ARID domain of KDM5A displays DNA binding activity with preference for the CCGCCC motif (53). These findings support the notion that KDM5A can directly target specific sites on chromatin, followed by recruitment of SIN3B-HDAC and NuRD complexes to integrate their enzymatic activities. When viewed in this way, KDM5A may not be a stable component of either the SIN3B-HDAC or the NuRD complex, and its association with these complexes may reflect the intimate interactions on chromatin. Thus, the results of our sucrose gradient analysis (Fig. 2*A*), in which KDM5A was primarily found to exist as a free form, although a small fraction appeared to stably associate with the SIN3B and NuRD complexes, may be due in part to its direct association with chromatin.

Because tri-methylated H3K4 (H3K4me3) preferentially occurs at the TSS of active genes, KDM5 family demethylase activity for H3K4me3 is hypothesized to negatively regulate transcription initiation. In fact, our analysis of two target gene loci, *GDF15* and *KLF2*, demonstrated that their transcriptional up-regulation following treatment with KDM5A siRNA was correlated with increased levels of H3K4me2/3. However, results of the microarray analysis revealed that hundreds of genes were down-regulated upon KDM5A depletion (Figs. 4 and 5). A similar positive effect on transcriptional activity was also demonstrated for LID, the KDM5A homologue in *Drosophila* (54). Further studies are needed to clarify the role of the KDM5 proteins on transcriptional regulation.

Acknowledgments—We thank Dr. Y. Kumaki for critical experimental advice, the Caenorhabditis Genetics Center, which is funded by National Institutes of Health, NCRR, and the National Bioresource Project for strains.

REFERENCES

1. Defeo-Jones, D., Huang, P. S., Jones, R. E., Haskell, K. M., Vuocolo, G. A., Hanobik, M. G., Huber, H. E., and Oliff, A. (1991) Cloning of cDNAs for cellular proteins that bind to the retinoblastoma gene product. *Nature* **352,** 251–254
2. Benevolenskaya, E. V., Murray, H. L., Branton, P., Young, R. A., and Kaelin, W. G., Jr. (2005) Binding of pRB to the PHD protein RBP2 promotes cellular differentiation. *Mol. Cell* **18,** 623–635
3. Klose, R. J., Yan, Q., Tothova, Z., Yamane, K., Erdjument-Bromage, H., Tempst, P., Gilliland, D. G., Zhang, Y., and Kaelin, W. G., Jr. (2007) The retinoblastoma binding protein RBP2 is an H3K4 demethylase. *Cell* **128,** 889–900
4. Nijwening, J. H., Geutjes, E. J., Bernards, R., and Beijersbergen, R. L. (2011) The histone demethylase Jarid1b (Kdm5b) is a novel component of the Rb pathway and associates with E2f-target genes in MEFs during senescence. *PLoS One* **6,** e25235
5. Chicas, A., Kapoor, A., Wang, X., Aksoy, O., Evertts, A. G., Zhang, M. Q., Garcia, B. A., Bernstein, E., and Lowe, S. W. (2012) H3K4 demethylation by Jarid1a and Jarid1b contributes to retinoblastoma-mediated gene silencing during cellular senescence. *Proc. Natl. Acad. Sci. U.S.A.* **109,** 8971–8976
6. Sharma, S. V., Lee, D. Y., Li, B., Quinlan, M. P., Takahashi, F., Maheswaran, S., McDermott, U., Azizian, N., Zou, L., Fischbach, M. A., Wong, K. K., Brandstetter, K., Wittner, B., Ramaswamy, S., Classon, M., and Settleman, J. (2010) A chromatin-mediated reversible drug-tolerant state in cancer cell subpopulations. *Cell* **141,** 69–80
7. Roesch, A., Fukunaga-Kalabis, M., Schmidt, E. C., Zabierowski, S. E., Brafford, P. A., Vultur, A., Basu, D., Gimotty, P., Vogt, T., and Herlyn, M. (2010) A temporarily distinct subpopulation of slow-cycling melanoma cells is required for continuous tumor growth. *Cell* **141,** 583–594
8. Lin, W., Cao, J., Liu, J., Beshiri, M. L., Fujiwara, Y., Francis, J., Cherniack, A. D., Geisen, C., Blair, L. P., Zou, M. R., Shen, X., Kawamori, D., Liu, Z., Grisanzio, C., Watanabe, H., Minamishima, Y. A., Zhang, Q., Kulkarni,

R. N., Signoretti, S., Rodig, S. J., Bronson, R. T., Orkin, S. H., Tuck, D. P., Benevolenskaya, E. V., Meyerson, M., Kaelin, W. G., Jr., and Yan, Q. (2011) Loss of the retinoblastoma binding protein 2 (RBP2) histone demethylase suppresses tumorigenesis in mice lacking Rb1 or Men1. *Proc. Natl. Acad. Sci. U.S.A.* **108,** 13379–13386
9. DiTacchio, L., Le, H. D., Vollmers, C., Hatori, M., Witcher, M., Secombe, J., and Panda, S. (2011) Histone lysine demethylase JARID1a activates CLOCK-BMAL1 and influences the circadian clock. *Science* **333,** 1881–1885
10. Lopez-Bigas, N., Kisiel, T. A., Dewaal, D. C., Holmes, K. B., Volkert, T. L., Gupta, S., Love, J., Murray, H. L., Young, R. A., and Benevolenskaya, E. V. (2008) Genome-wide analysis of the H3K4 histone demethylase RBP2 reveals a transcriptional program controlling differentiation. *Mol. Cell* **31,** 520–530
11. Yamane, K., Tateishi, K., Klose, R. J., Fang, J., Fabrizio, L. A., Erdjument-Bromage, H., Taylor-Papadimitriou, J., Tempst, P., and Zhang, Y. (2007) PLU-1 is an H3K4 demethylase involved in transcriptional repression and breast cancer cell proliferation. *Mol. Cell* **25,** 801–812
12. Dey, B. K., Stalker, L., Schnerch, A., Bhatia, M., Taylor-Papidimitriou, J., and Wynder, C. (2008) The histone demethylase KDM5b/JARID1b plays a role in cell fate decisions by blocking terminal differentiation. *Mol. Cell. Biol.* **28,** 5312–5327
13. Schmitz, S. U., Albert, M., Malatesta, M., Morey, L., Johansen, J. V., Bak, M., Tommerup, N., Abarrategui, I., and Helin, K. (2011) Jarid1b targets genes regulating development and is involved in neural differentiation. *EMBO J.* **30,** 4586–4600
14. Iwase, S., Lan, F., Bayliss, P., de la Torre-Ubieta, L., Huarte, M., Qi, H. H., Whetstine, J. R., Bonni, A., Roberts, T. M., and Shi, Y. (2007) The X-linked mental retardation gene SMCX/JARID1C defines a family of histone H3 lysine 4 demethylases. *Cell* **128,** 1077–1088
15. Wang, W., Meadows, L. R., den Haan, J. M., Sherman, N. E., Chen, Y., Blokland, E., Shabanowitz, J., Agulnik, A. I., Hendrickson, R. C., and Bishop, C. E. (1995) Human H-Y: a male-specific histocompatibility antigen derived from the SMCY protein. *Science* **269,** 1588–1590
16. Scott, D. M., Ehrmann, I. E., Ellis, P. S., Bishop, C. E., Agulnik, A. I., Simpson, E., and Mitchell, M. J. (1995) Identification of a mouse male-specific transplantation antigen, H-Y. *Nature* **376,** 695–698
17. Christensen, J., Agger, K., Cloos, P. A., Pasini, D., Rose, S., Sennels, L., Rappsilber, J., Hansen, K. H., Salcini, A. E., and Helin, K. (2007) RBP2 belongs to a family of demethylases, specific for tri-and dimethylated lysine 4 on histone 3. *Cell* **128,** 1063–1076
18. Li, L., Greer, C., Eisenman, R. N., and Secombe, J. (2010) Essential functions of the histone demethylase lid. *PLoS Genet.* **6,** e1001221
19. Di Stefano, L., Walker, J. A., Burgio, G., Corona, D. F., Mulligan, P., Näär, A. M., and Dyson, N. J. (2011) Functional antagonism between histone H3K4 demethylases *in vivo*. *Genes Dev.* **25,** 17–28
20. Eissenberg, J. C., Lee, M. G., Schneider, J., Ilvarsonn, A., Shiekhattar, R., and Shilatifard, A. (2007) The trithorax-group gene in *Drosophila* little imaginal discs encodes a trimethylated histone H3 Lys4 demethylase. *Nat. Struct. Mol. Biol.* **14,** 344–346
21. Lee, N., Erdjument-Bromage, H., Tempst, P., Jones, R. S., and Zhang, Y. (2009) The H3K4 demethylase lid associates with and inhibits histone deacetylase Rpd3. *Mol. Cell. Biol.* **29,** 1401–1410
22. Hayakawa, T., Ohtani, Y., Hayakawa, N., Shinmyozu, K., Saito, M., Ishikawa, F., and Nakayama, J. (2007) RBP2 is an MRG15 complex component and down-regulates intragenic histone H3 lysine 4 methylation. *Genes Cells* **12,** 811–826
23. Suganuma, T., and Workman, J. L. (2008) Crosstalk among histone modifications. *Cell* **135,** 604–607
24. Hayakawa, T., and Nakayama, J. (2011) Physiological roles of class I HDAC complex and histone demethylase. *J. Biomed. Biotechnol.* 2011, 129383
25. Zhang, P., Du, J., Sun, B., Dong, X., Xu, G., Zhou, J., Huang, Q., Liu, Q., Hao, Q., and Ding, J. (2006) Structure of human MRG15 chromo domain and its binding to Lys36-methylated histone H3. *Nucleic Acids Res.* **34,** 6621–6628
26. Moshkin, Y. M., Kan, T. W., Goodfellow, H., Bezstarosti, K., Maeda, R. K., Pilyugin, M., Karch, F., Bray, S. J., Demmers, J. A., and Verrijzer, C. P. (2009) Histone chaperones ASF1 and NAP1 differentially modulate removal of active histone marks by LID-RPD3 complexes during NOTCH silencing. *Mol. Cell* **35,** 782–793
27. Knoepfler, P. S., and Eisenman, R. N. (1999) Sin meets NuRD and other tails of repression. *Cell* **99,** 447–450
28. Denslow, S. A., and Wade, P. A. (2007) The human Mi-2/NuRD complex and gene regulation. *Oncogene* **26,** 5433–5438
29. Xue, Y., Wong, J., Moreno, G. T., Young, M. K., Côté, J., and Wang, W. (1998) NURD, a novel complex with both ATP-dependent chromatin-remodeling and histone deacetylase activities. *Mol. Cell* **2,** 851–861
30. Wade, P. A., Jones, P. L., Vermaak, D., and Wolffe, A. P. (1998) A multiple subunit Mi-2 histone deacetylase from *Xenopus laevis* cofractionates with an associated Snf2 superfamily ATPase. *Curr. Biol.* **8,** 843–846
31. Tong, J. K., Hassig, C. A., Schnitzler, G. R., Kingston, R. E., and Schreiber, S. L. (1998) Chromatin deacetylation by an ATP-dependent nucleosome remodelling complex. *Nature* **395,** 917–921
32. Zhang, Y., LeRoy, G., Seelig, H. P., Lane, W. S., and Reinberg, D. (1998) The dermatomyositis-specific autoantigen Mi2 is a component of a complex containing histone deacetylase and nucleosome remodeling activities. *Cell* **95,** 279–289
33. Ahringer, J. (2000) NuRD and SIN3 histone deacetylase complexes in development. *Trends Genet.* **16,** 351–356
34. McDonel, P., Costello, I., and Hendrich, B. (2009) Keeping things quiet: roles of NuRD and Sin3 co-repressor complexes during mammalian development. *Int. J. Biochem. Cell Biol.* **41,** 108–116
35. Lai, A. Y., and Wade, P. A. (2011) Cancer biology and NuRD: a multifaceted chromatin remodelling complex. *Nat. Rev. Cancer* **11,** 588–596
36. Hiragami-Hamada, K., Shinmyozu, K., Hamada, D., Tatsu, Y., Uegaki, K., Fujiwara, S., and Nakayama, J. (2011) N-terminal phosphorylation of HP1α promotes its chromatin binding. *Mol. Cell. Biol.* **31,** 1186–1200
37. Hayakawa, T., Zhang, F., Hayakawa, N., Ohtani, Y., Shinmyozu, K., Nakayama, J., and Andreassen, P. R. (2010) MRG15 binds directly to PALB2 and stimulates homology-directed repair of chromosomal breaks. *J. Cell Sci.* **123,** 1124–1130
38. Brenner, S. (1974) The genetics of *Caenorhabditis elegans*. *Genetics* **77,** 71–94
39. Hughes-Davies, L., Huntsman, D., Ruas, M., Fuks, F., Bye, J., Chin, S. F., Milner, J., Brown, L. A., Hsu, F., Gilks, B., Nielsen, T., Schulzer, M., Chia, S., Ragaz, J., Cahn, A., Linger, L., Ozdag, H., Cattaneo, E., Jordanova, E. S., Schuuring, E., Yu, D. S., Venkitaraman, A., Ponder, B., Doherty, A., Aparicio, S., Bentley, D., Theillet, C., Ponting, C. P., Caldas, C., and Kouzarides, T. (2003) EMSY links the BRCA2 pathway to sporadic breast and ovarian cancer. *Cell* **115,** 523–535
40. Malovannaya, A., Lanz, R. B., Jung, S. Y., Bulynko, Y., Le, N. T., Chan, D. W., Ding, C., Shi, Y., Yucer, N., Krenciute, G., Kim, B. J., Li, C., Chen, R., Li, W., Wang, Y., O'Malley, B. W., and Qin, J. (2011) Analysis of the human endogenous coregulator complexome. *Cell* **145,** 787–799
41. Ferguson, E. L., and Horvitz, H. R. (1989) The multivulva phenotype of certain *Caenorhabditis elegans* mutants results from defects in two functionally redundant pathways. *Genetics* **123,** 109–121
42. Fay, D. S., and Yochem, J. (2007) The SynMuv genes of *Caenorhabditis elegans* in vulval development and beyond. *Dev. Biol.* **306,** 1–9
43. Ceol, C. J., Stegmeier, F., Harrison, M. M., and Horvitz, H. R. (2006) Identification and classification of genes that act antagonistically to let-60 Ras signaling in *Caenorhabditis elegans* vulval development. *Genetics* **173,** 709–726
44. Solari, F., and Ahringer, J. (2000) NURD-complex genes antagonise Ras-induced vulval development in *Caenorhabditis elegans*. *Curr. Biol.* **10,** 223–226
45. Li, Q., Shi, L., Gui, B., Yu, W., Wang, J., Zhang, D., Han, X., Yao, Z., and Shang, Y. (2011) Binding of the JmjC demethylase JARID1B to LSD1/NuRD suppresses angiogenesis and metastasis in breast cancer cells by repressing chemokine CCL14. *Cancer Res.* **71,** 6899–6908
46. Barrett, A., Madsen, B., Copier, J., Lu, P. J., Cooper, L., Scibetta, A. G., Burchell, J., and Taylor-Papadimitriou, J. (2002) PLU-1 nuclear protein, which is upregulated in breast cancer, shows restricted expression in normal human adult tissues: a new cancer/testis antigen? *Int. J. Cancer* **101,** 581–588
47. Albert, M., Schmitz, S. U., Kooistra, S. M., Malatesta, M., Morales Torres, C.,

Rekling, J. C., Johansen, J. V., Abarrategui, I., and Helin, K. (2013) The histone demethylase Jarid1b ensures faithful mouse development by protecting developmental genes from aberrant H3K4me3. *PLoS Genet.* **9,** e1003461
48. Wang, Y., Zhang, H., Chen, Y., Sun, Y., Yang, F., Yu, W., Liang, J., Sun, L., Yang, X., Shi, L., Li, R., Li, Y., Zhang, Y., Li, Q., Yi, X., and Shang, Y. (2009) LSD1 is a subunit of the NuRD complex and targets the metastasis programs in breast cancer. *Cell* **138,** 660–672
49. Whyte, W. A., Bilodeau, S., Orlando, D. A., Hoke, H. A., Frampton, G. M., Foster, C. T., Cowley, S. M., and Young, R. A. (2012) Enhancer decommissioning by LSD1 during embryonic stem cell differentiation. *Nature* **482,** 221–225
50. Chaturvedi, C. P., Somasundaram, B., Singh, K., Carpenedo, R. L., Stanford, W. L., Dilworth, F. J., and Brand, M. (2012) Maintenance of gene silencing by the coordinate action of the H3K9 methyltransferase G9a/KMT1C and the H3K4 demethylase Jarid1a/KDM5A. *Proc. Natl. Acad. Sci. U.S.A.* **109,** 18845–18850
51. von Zelewsky, T., Palladino, F., Brunschwig, K., Tobler, H., Hajnal, A., and Müller, F. (2000) The *C. elegans* Mi-2 chromatin-remodelling proteins function in vulval cell fate determination. *Development* **127,** 5277–5284
52. Wang, G. G., Song, J., Wang, Z., Dormann, H. L., Casadio, F., Li, H., Luo, J. L., Patel, D. J., and Allis, C. D. (2009) Haematopoietic malignancies caused by dysregulation of a chromatin-binding PHD finger. *Nature* **459,** 847–851
53. Tu, S., Teng, Y. C., Yuan, C., Wu, Y. T., Chan, M. Y., Cheng, A. N., Lin, P. H., Juan, L. J., and Tsai, M. D. (2008) The ARID domain of the H3K4 demethylase RBP2 binds to a DNA CCGCCC motif. *Nat. Struct. Mol. Biol.* **15,** 419–421
54. Lloret-Llinares, M., Pérez-Lluch, S., Rossell, D., Morán, T., Ponsa-Cobas, J., Auer, H., Corominas, M., and Azorín, F. (2012) dKDM5/LID regulates H3K4me3 dynamics at the transcription-start site (TSS) of actively transcribed developmental genes. *Nucleic Acids Res.* **40,** 9493–9505